Supplementary Information (SI) for Sustainable Energy & Fuels.
This journal is © The Royal Society of Chemistry 2025

Fusion of Nitro Isomers of Naphthoquinone Enhances Capacity and Cyclability in Zn-ion Batteries

Supporting information

S.1. Materials and characterisation:

98% pure 2,3-dichloro-1,4-naphthoquinone (DCNQ) was obtained from TCI chemicals. Sulfuric acid and nitric acid were purchased from Thermo Fisher Scientific. Super P carbon and PVDF were from Alfa Aesar Pvt. Ltd. Nafion ionomer solution (5 wt. %) and $Zn(OTf)_2$ were purchased from Sigma-Aldrich. All chemicals were used as received. ^1H NMR of all active materials was recorded in 99% deuterated solvent or $CDCl_3$, purchased from Sigma-Aldrich, using a Bruker NMR spectrometer at 400 MHz. Melting points of the compounds were obtained by using the G LAB apparatus, and they were 145 °C (± 4), 175 °C (± 3), and 170 °C (± 3) for 5-nitro 2,3-dichloro 1,4-naphthoquinone (5-DCNNQ), 6-nitro 2,3-dichloro 1,4-naphthoquinone (6-DCNNQ) and their mixture DCNNQmix, respectively. 5-DCNNQ crystals were obtained from a saturated solution of 5-DCNNQ in methanol (at 50 °C) upon slowly cooling to room temperature, yielding colourless needle-like crystals. Single crystal X-ray diffraction was performed using Bruker D8 Venture diffractometer with PHOTON II detector operated with a molybdenum (λ(MoKα) = 0.71073 Å) X-ray radiation. For structure solving, more than 4292 reflections are considered. APEX3-SAINT program (Bruker AXS) and SADABS program were used for preliminary determination of the cell constants, data collection, data refinement, and an absorption correction, respectively [1]. The data were acquired at 173 K, and the space group determination and structure solution was carried out using the SHELXT-2018/2 and SHELXL-2018/3 programs [2]. ORTEP-3 [3] for windows was used to draw the structure.

S.2. Synthesis procedure of 5-nitro 2,3-dichloro 1,4-naphthoquinone (5-DCNNQ), 6-nitro 2,3-dichloro 1,4-naphthoquinone (6-DCNNQ):

The preparation 5/6-DCNNQ was done according to the literature report [4]. A mixture of fuming HNO_3 (4.5 gm) and H_2SO_4 (15 gm) was prepared in an ice bath. DCNQ (1.5 g, 0.66 mmol) was slowly added to the prepared solution and then heated at 80°C for 3 h. A dark brown solution was poured into the ice water (100 mL) to give a bright yellow precipitate. This yellow solid was filtered and washed with water and then collected by vacuum filtration. Column chromatography with ethyl acetate: hexane of 60:40 was used to separate the final product 5-DCNNQ (~ 69%, major) and 6-DCNNQ (~ 30%, minor).

5-DCNNQ: ^{1}H NMR ($CDCl_3$, 500 MHz): δ 8.41 (d, 1H,), 7.98 (t, ^{1}H), 7.79 (d, 1H) pp. 6-DCNNQ: ^{1}H NMR ($CDCl_3$, 500 MHz): δ 9.00 (d, 1H), 8.62 (dd, 1H), 8.42 (d, 1H).

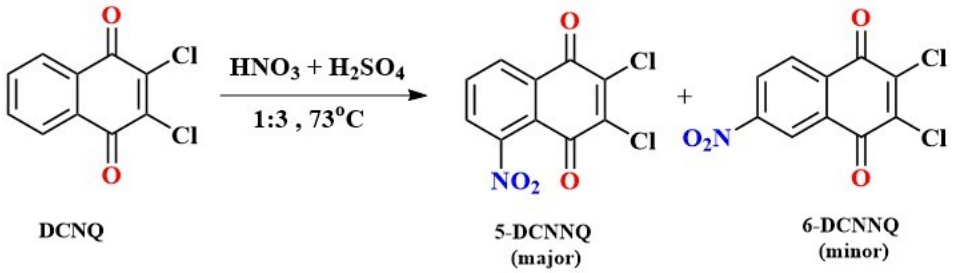

Scheme S1. Synthesis scheme of 5-DCNNQ and 6-DCNNQ.

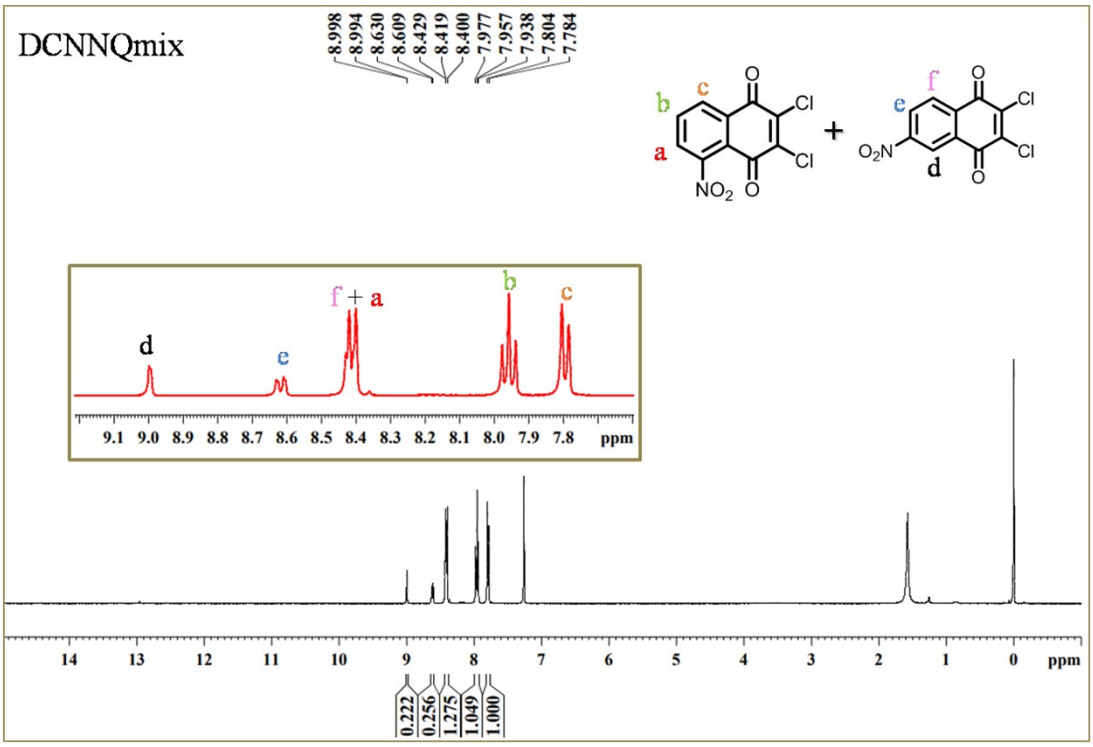

Fig. S1. [1]H-NMR of the reaction mixture (DCNNQmix).

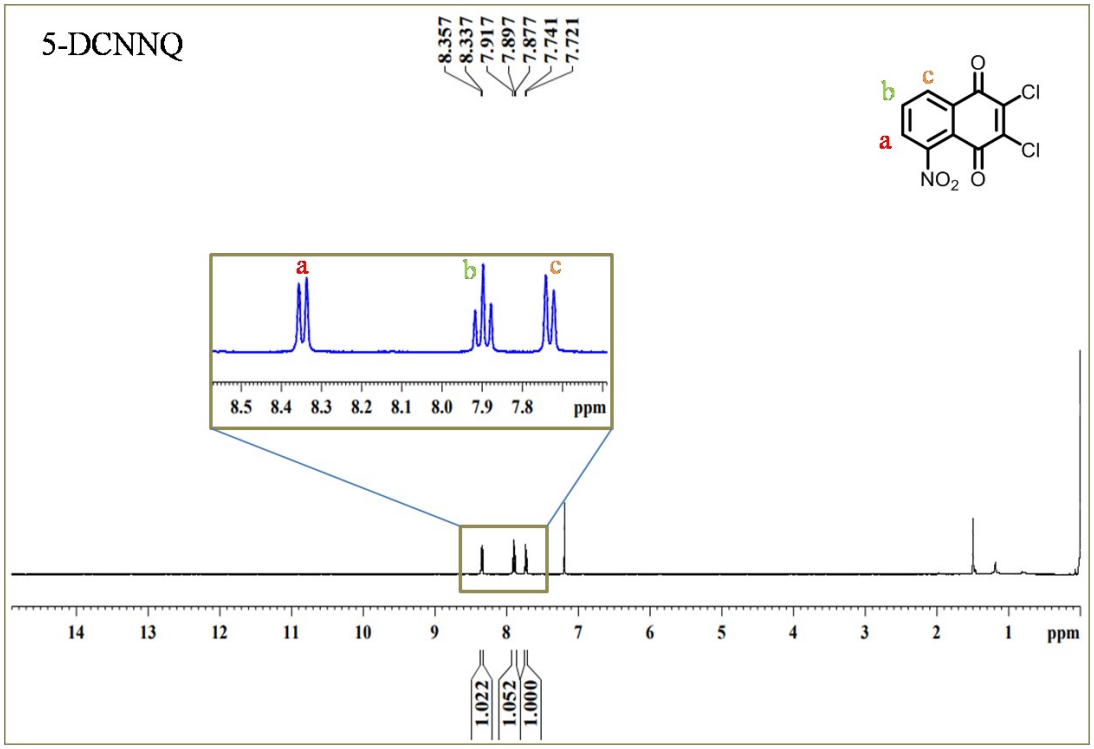

Fig. S2. [1]H-NMR of 5-DCNNQ.

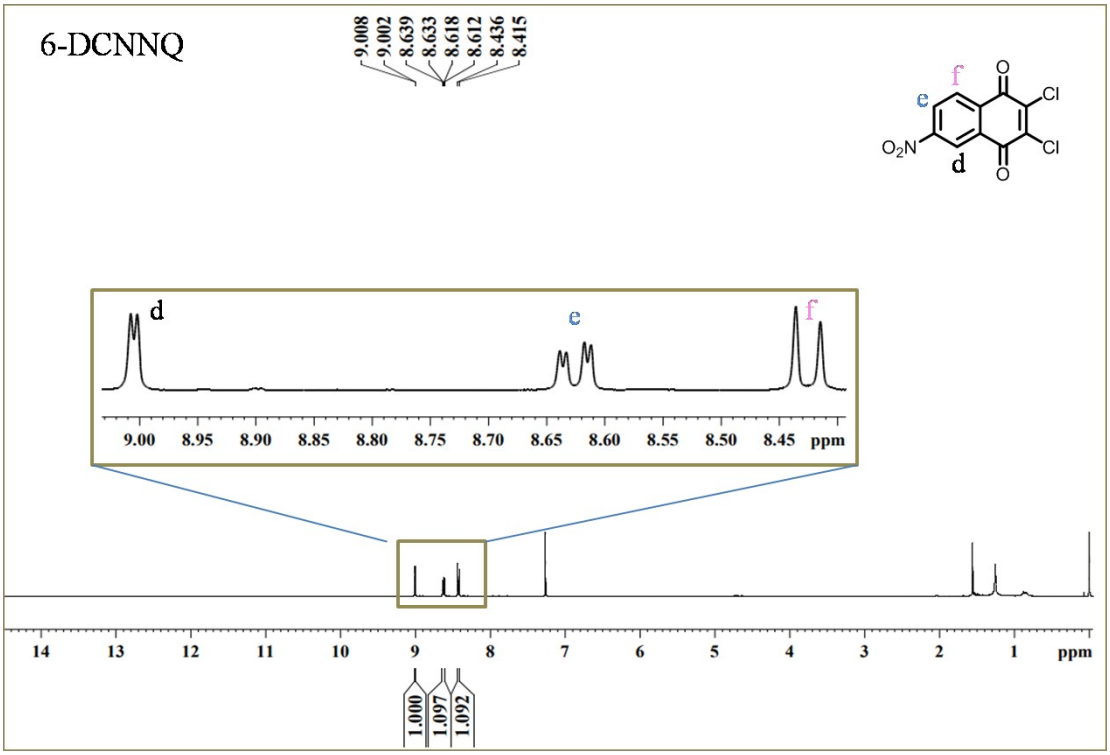

Fig. S3. ^{1}H-NMR of 6-DCNNQ.

Table S1. Crystal structure parameters of 5-DCNNQ at low temperature.

CCDC number	2325245
Space group	P 2_1 / c
Crystal symmetry	Monoclinic
Cell parameters	a=9.1782 (18), b=14.990 (3), c=7.7606 (13) α = 90°, β = 102.925° (6), γ = 90° V = 1040.7 Å Z = 4 Density = 1.736 g cm^{-3} R = 0.078

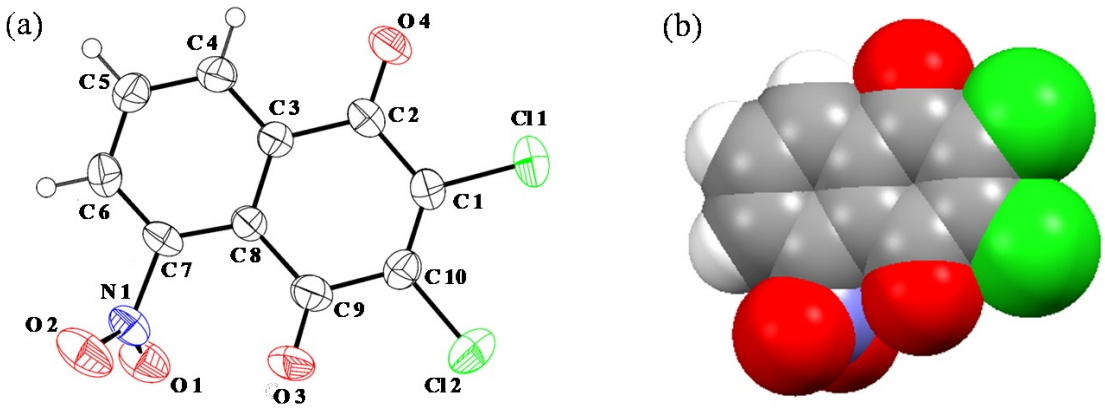

Fig. S4. Crystal structure of 5-DCNNQ **(a)** ORTEP diagram and **(b)** space fill form.

Fig. S5. Solubility tests of powder samples of 5-DCNNQ, DCNNQmix, and 6-DCNNQ in the electrolyte.

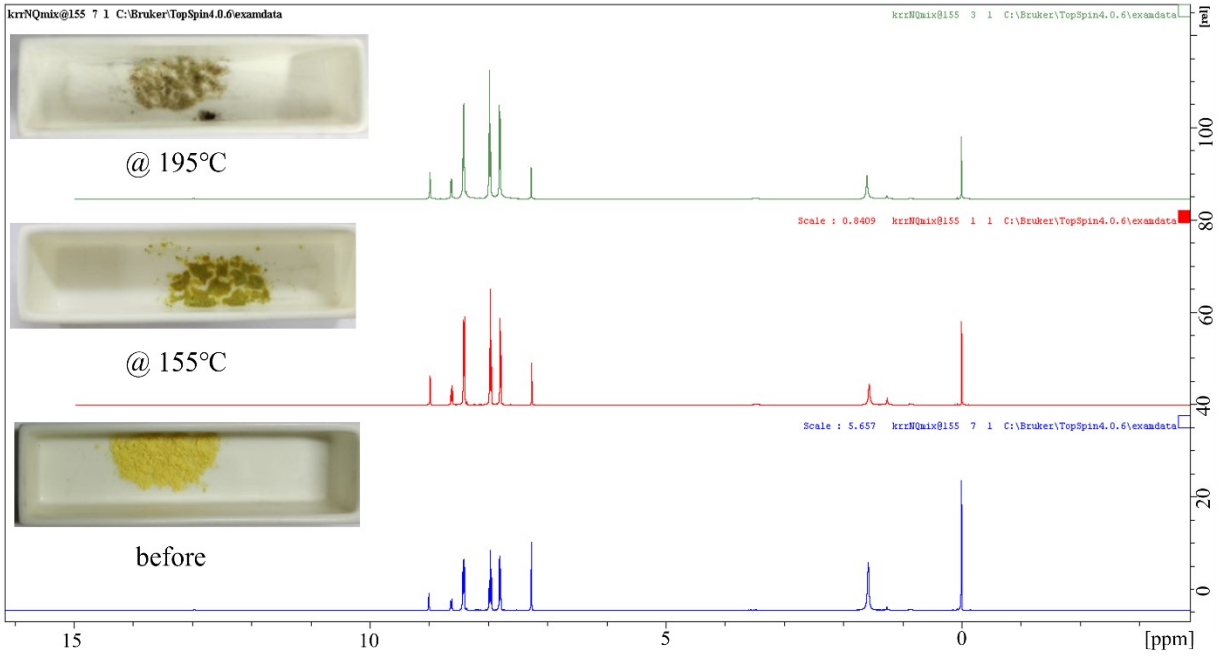

Fig. S6. A comparative ^{1}H-NMR of DCNNQmix before and after heating at 155 °C and 195 °C.

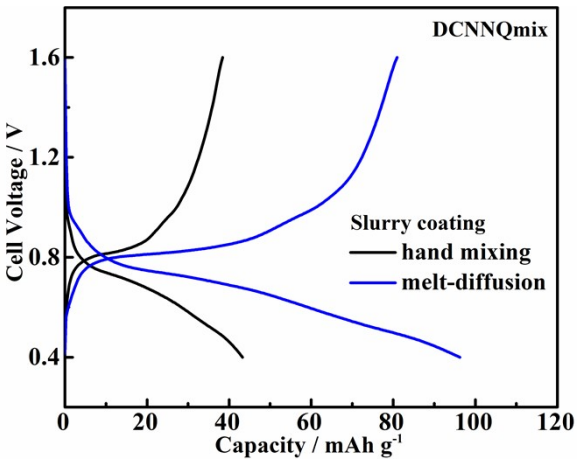

Fig. S7. Comparative charge-discharge plot (10th cycle) of Zn//DCNNQmix-Cathode cell at 0.1 A g^{-1} of current density when slurry made with hand mixing and melt-diffusion technique.

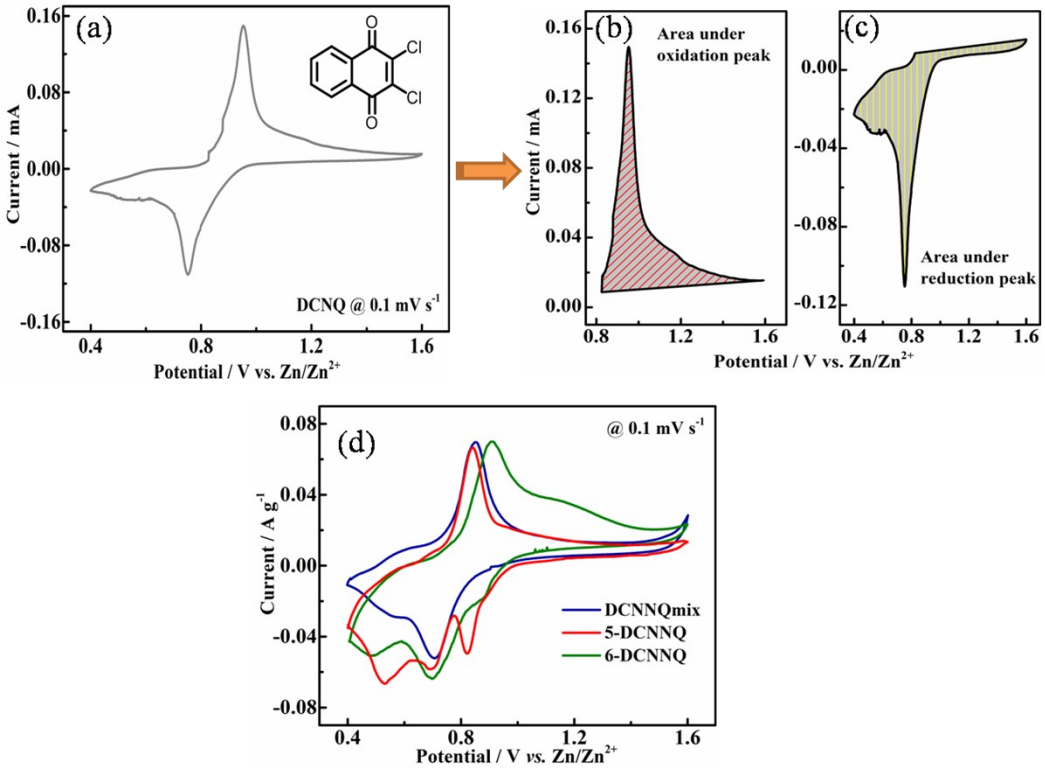

Fig. S8. Cyclic voltammetry (CV) of **(a)** DCNQ-Cathode recorded and its area under the **(b)** oxidation and **(c)** reduction peak at the scan rate of 0.1 mV s^{-1}. **(d)** Comparative CV curve of 5-DCNNQ-Cathode, 6-DCNNQ-Cathode, and DCNNQmix-Cathode in two-electrode mode at the scan rate of 0.1 mV s^{-1}.

Table S2. Depicts the area under the reduction and oxidation peaks and their ratio of 5- and 6-DCNNQ-Cathode and DCNNQmix-Cathode.

Electrode	**Area under reduction peak (A_R) /mW**	**Area under oxidation peak (A_o)/ mW**	**Ratio (A_R /A_o)**
DCNQ	2.316×10^{-2}	1.944×10^{-2}	1.19
5-DCNNQ	4.715×10^{-2}	1.269×10^{-2}	3.7
6-DCNNQ	3.885×10^{-2}	1.553×10^{-2}	2.5
DCNNQmix	2.063×10^{-2}	8.203×10^{-3}	2.5

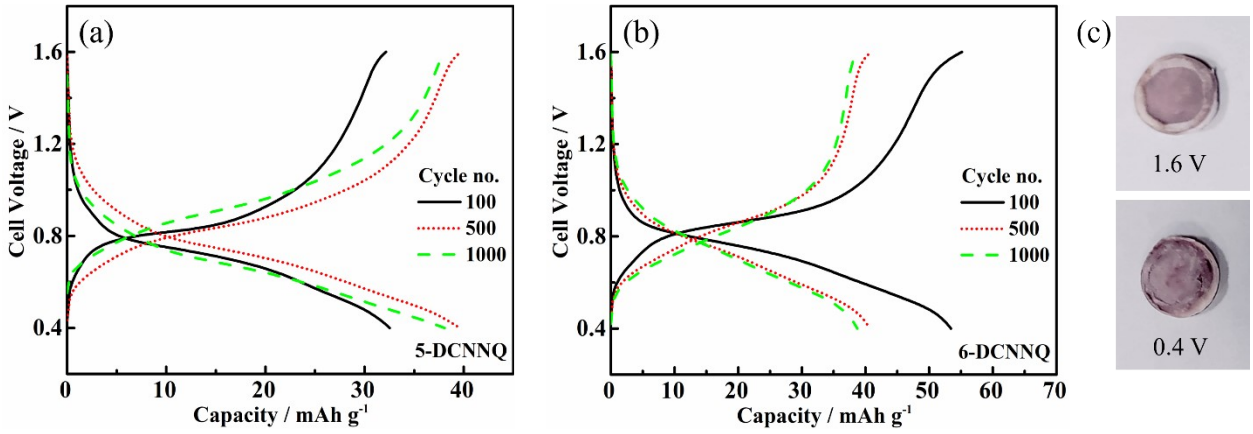

Fig. S9. Galvanostatic charge-discharge plot of **(a)** 5-DCNNQ-Cathode and **(b)** 6-DCNNQ-Cathode at the rate of 0.1 A g^{-1}. **(c)** Photographic image of GF membrane at 1.6 V and 0.4 V recovered after disassembling the Zn//DCNNQmix cell.

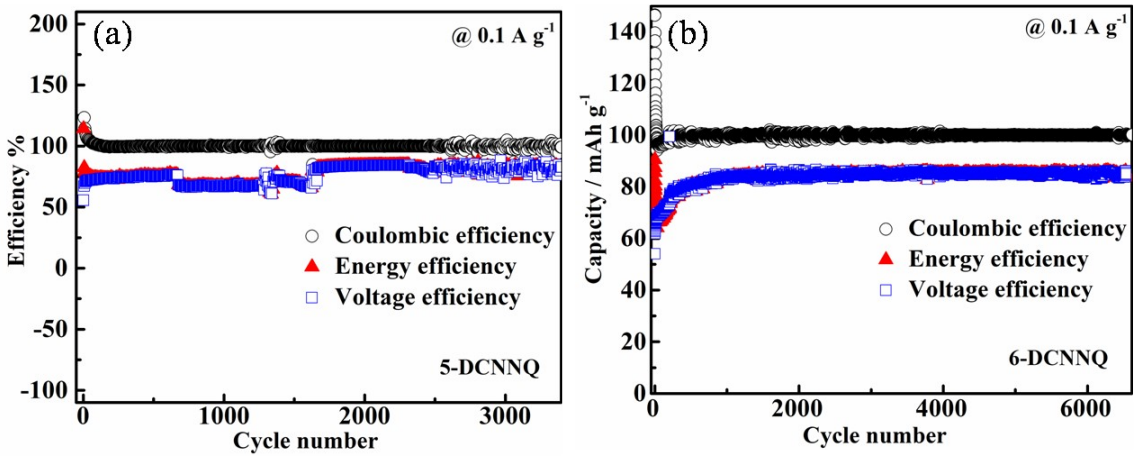

Fig. S10. Efficiency plot of **(a)** 5-DCNNQ-Cathode and **(b)** 6-DCNNQ-Cathode at the current density of 0.1 A g^{-1}.

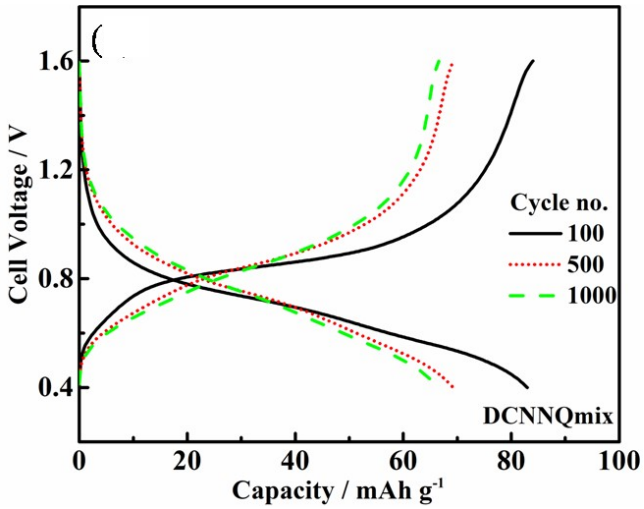

Fig. S11. Charge-discharge curve of DCNNQmix-PVDF cycled at the rate of 0.1 A g^{-1}.

Table S3. Representation of unit charges experienced by >C=O and $–NO_2$ groups in 5-DCNNQ and 6-DCNNQ calculated using Natural Bond Orbital analysis.

Active materials	Charges at >C=O at neutral states		Charge differences when reduced by $1e^-$	
	at >C=O	at $-NO_2$	at >C=O	at $-NO_2$
5-DCNNQ	ortho = 0.518	0.517	ortho = -0.119	0.008
	far = 0.518		far = -0.125	
6-DCNNQ	meta = 0.519	0.513	meta = -0.094	-0.016
	para = 0.517		para = -0.123	

Table S4. The table compares the quinone-based organic cathode materials for Zn-ion batteries.

Active cathode materials	Conductive Carbon	Separator	Diffusion coefficient	Capacity / Capacity retention	Current density / Cycle number	Ref.
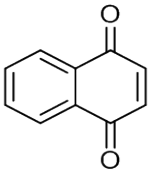 1,4-NQ	Super P	Nafion-212		50 mAh g^{-1} / 87%	0.02 A g^{-1} /	20
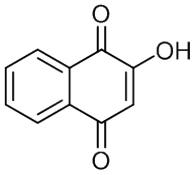 LS	Super P	Nafion-212	10^{-13} – 10^{-14} cm^2 s^{-1}	50 mAh g^{-1} / 50%	0.1 A g^{-1} / 500	19
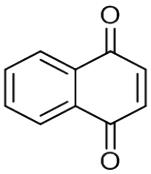 NQ@CNT	CNT	Glass Fiber		137.2 mAh g^{-1} / 41%	1 C / 1500	23
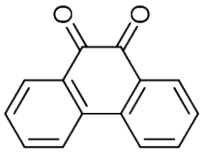 PQ@AC	Active Carbon	Glass Fiber	10^{-9} cm^2 s^{-1}	107.8 mAh g^{-1} / 96%	5 A g^{-1} / 36000	21
DCNNQmix	Super P	Glass Fiber	10^{-7} cm^2 s^{-1}	140 mAh g^{-1} / 91.3%	0.1 A g^{-1} / 9600	This work

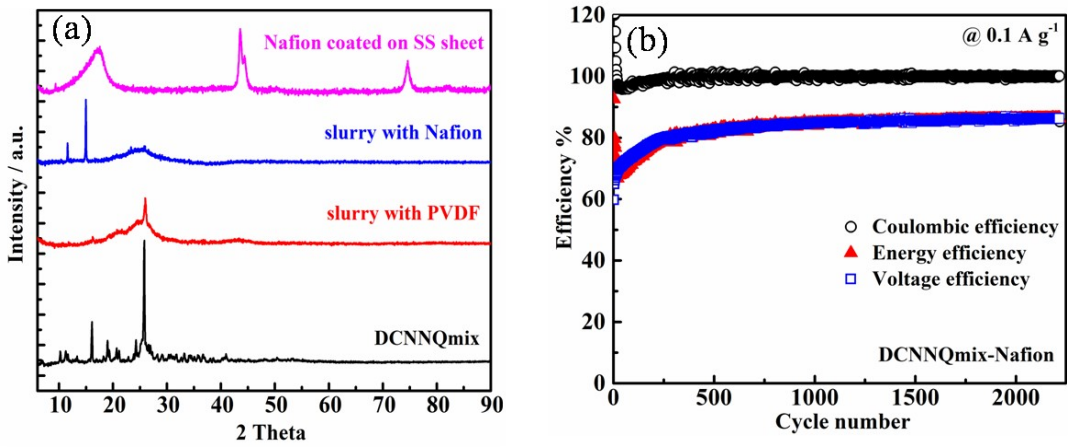

Fig. S12. (a) PowderXRD of DCNNQmix powder and its slurry with PVDF and Nafion binder, and Nafion solution coated on a stainless steel sheet. **(b)** Efficiency vs. cycle number plot of Nafion-based Zn//DCNNQ-Cathode for >2200 cycles at 0.1 A g^{-1}.

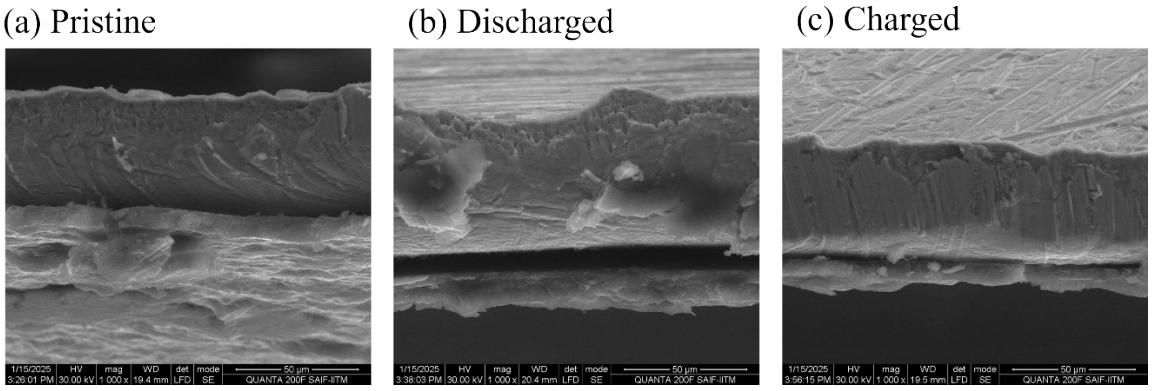

Fig. S13. HRSEM crosssection images of DCNNQ electrode at **(a)** pristine**, (b)** discharged, and **(c)** charged states.

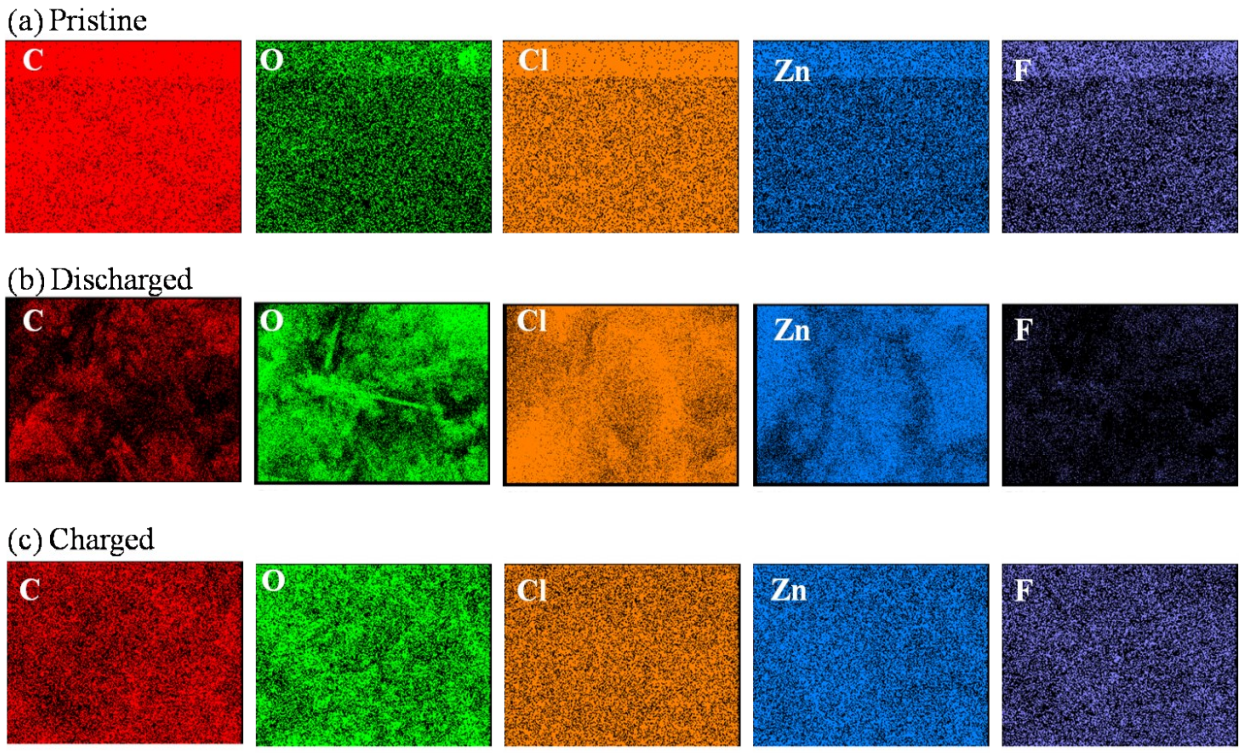

Fig. S14. HR-SEM coupled with EDX for elemental mapping of DCNNQmix electrodes at **(a)** pristine, **(b)** discharged, and **(c)** charged state of C, O, Cl, Zn, and F.

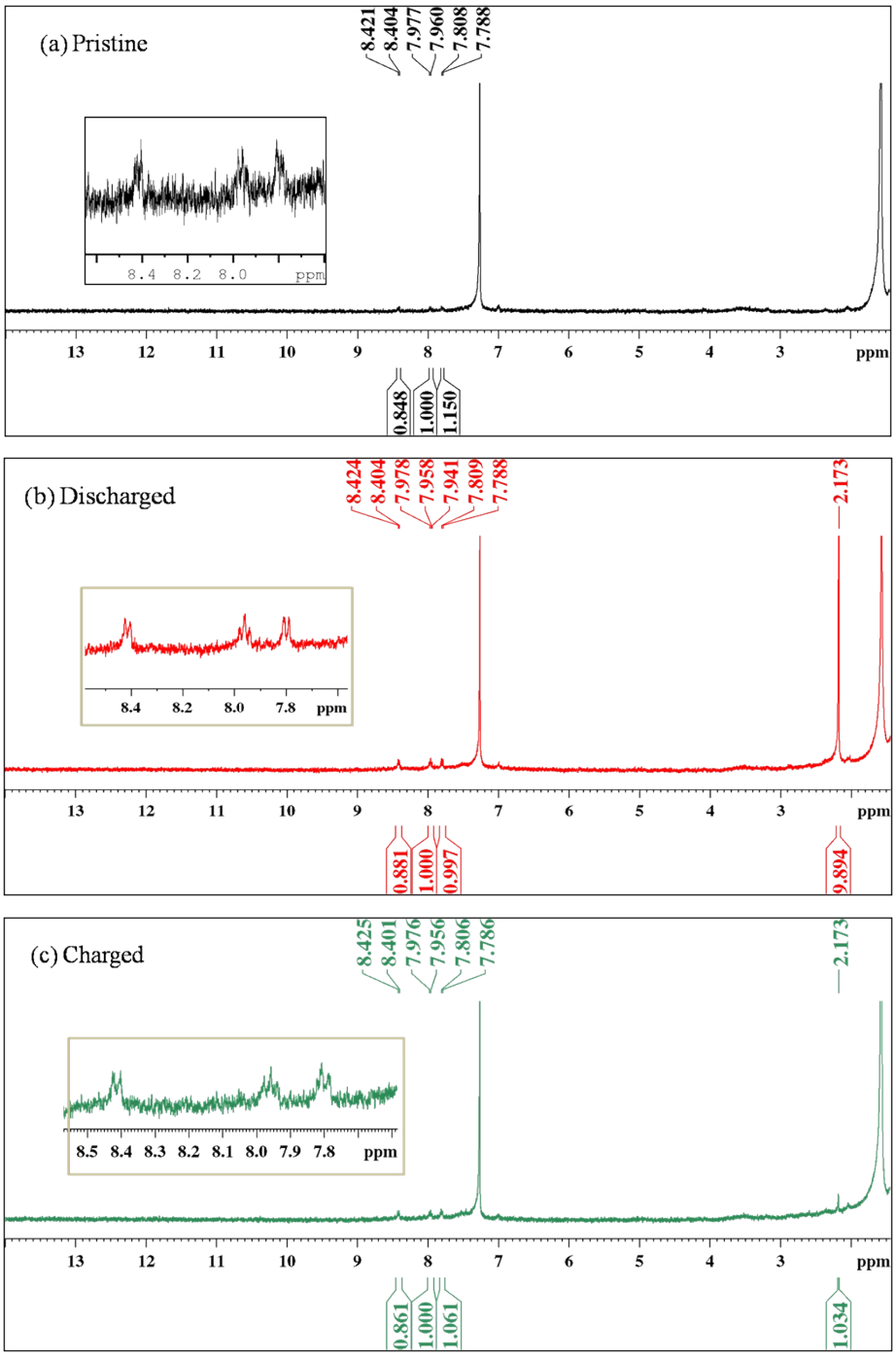

Fig. S15. ^{1}H-NMR of DCNNQmix extracted from the electrodes at **(a)** pristine, **(b)** discharged, and **(c)** charged state using $CDCl_3$.

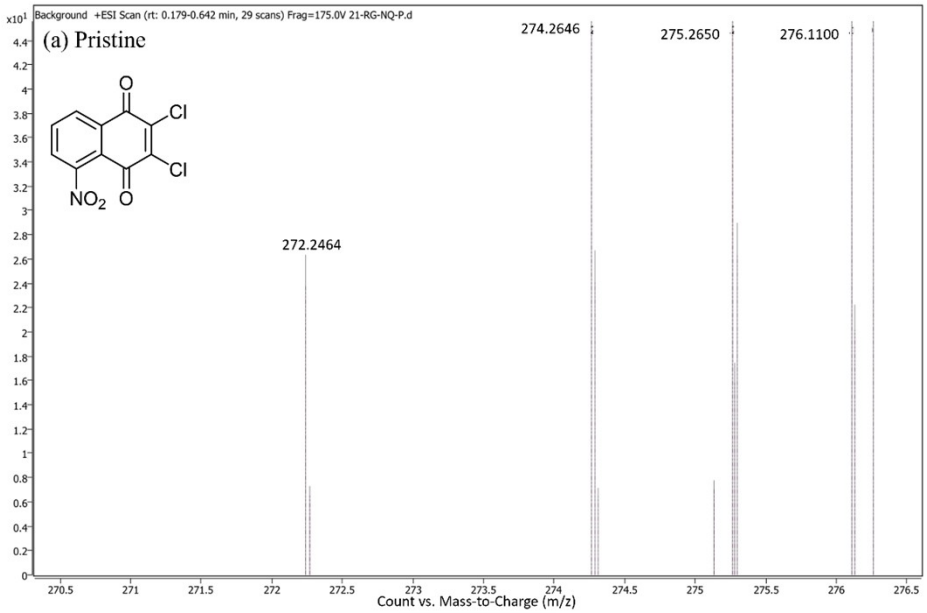
Background +ESI Scan (rt: 0.179-0.642 min, 29 scans) Frag=175.0V 21-RG-NQ-P.d
x10^1
(a) Pristine
274.2646
275.2650
276.1100
272.2464
Count vs. Mass-to-Charge (m/z)

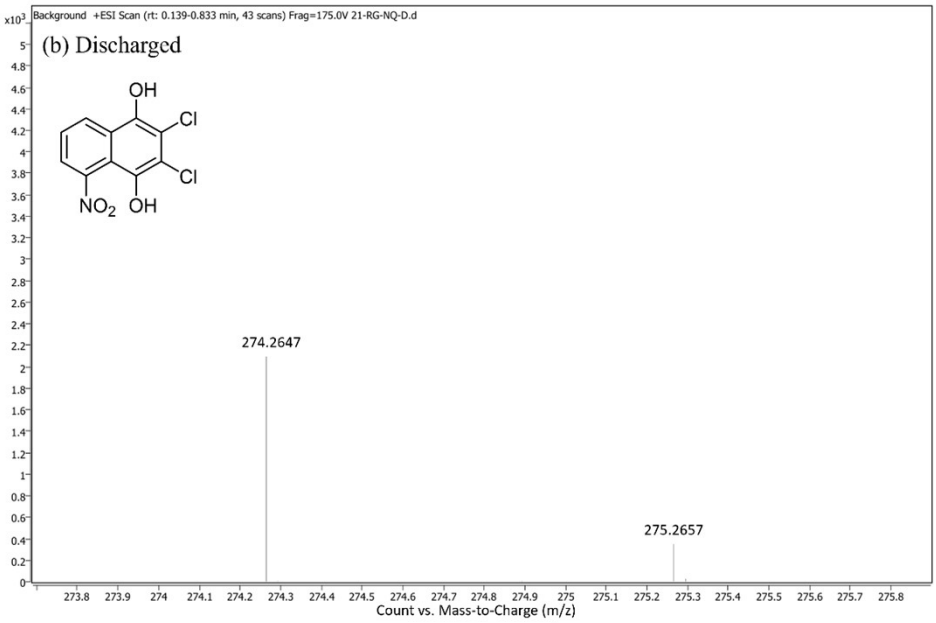
Background +ESI Scan (rt: 0.139-0.833 min, 43 scans) Frag=175.0V 21-RG-NQ-D.d
x10^3
(b) Discharged
274.2647
275.2657
Count vs. Mass-to-Charge (m/z)

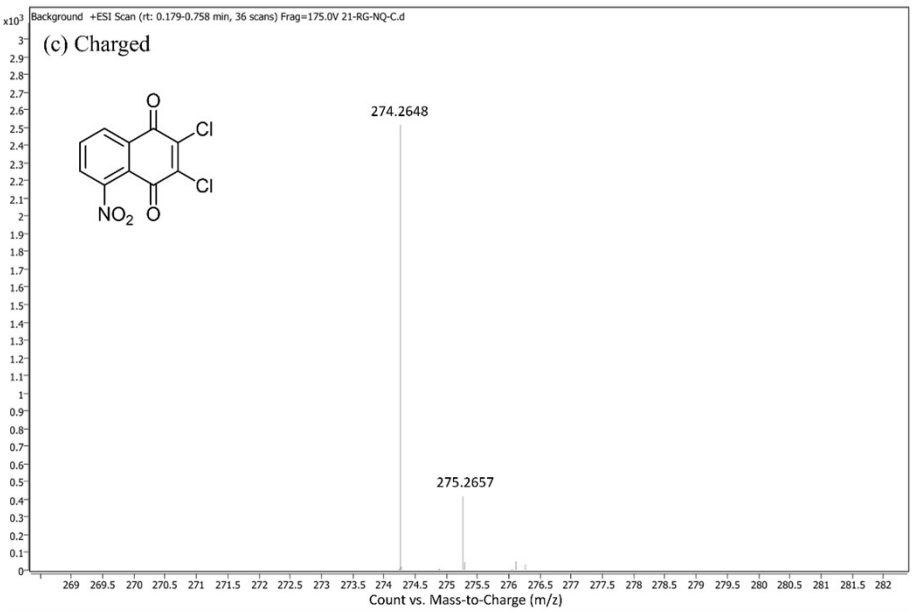

Fig. S16. Mass spectrum of DCNNQmix extracted from the electrodes at **(a)** pristine, **(b)** discharged, and **(c)** charged state.

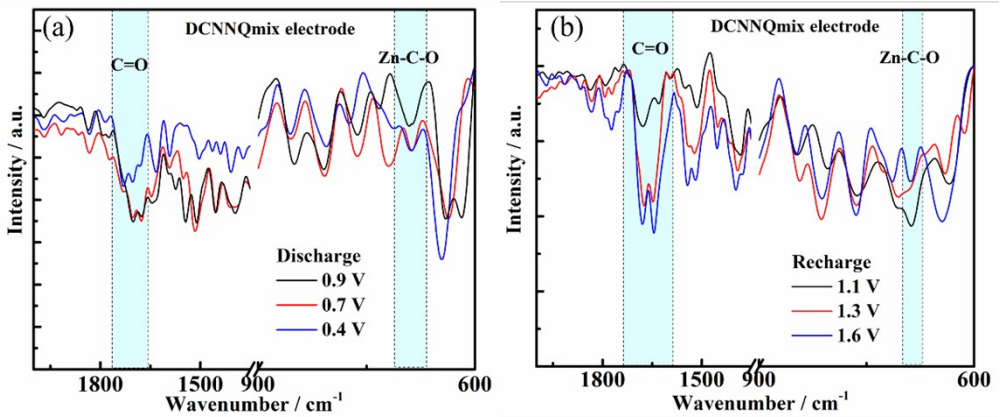

Fig. S17. ATR-IR recorded of DCNNQmix electrodes at various cell voltage during **(a)** discharge and **(b)** charge of the cell.

References

[1] G. M. Sheldrick, *Sadabs* **1996**.

[2] G. M. Sheldrick, *Acta Crystallogr. Sect. C Struct. Chem.* **2015**, *71*, 3–8.

[3] L. J. Farrugia, *J. Appl. Crystallogr.* **2012**, *45*, 849–854.

[4] E. G. Stoddard, B. J. Killinger, R. N. Nair, N. C. Sadler, R. F. Volk, S. O. Purvine, A. K. Shukla, J. N. Smith, A. T. Wright, *J. Am. Chem. Soc.* **2017**, *139*, 16032–16035.